The Mechanism of Islet Amyloid Polypeptide Toxicity Is Membrane Disruption by Intermediate-Sized Toxic Amyloid Particles

Juliette Janson, Richard H. Ashley, David Harrison, Susan McIntyre, and Peter C. Butler

NIDDM is characterized by islet amyloid deposits and decreased β-cell mass. Islet amyloid is derived from the locally expressed protein islet amyloid polypeptide (IAPP). While it is now widely accepted that abnormal aggregation of IAPP has a role in β-cell death in NIDDM, the mechanism remains unknown. We hypothesized that small IAPP aggregates, rather than mature large amyloid deposits, are cytotoxic. Consistent with this hypothesis, freshly dissolved human (h)-IAPP was cytotoxic when added to dispersed mouse and human islet cells, provoking the formation of abnormal vesicle-like membrane structures in association with vacuolization and cell death. Human islet cell death occurred by both apoptosis and necrosis, predominantly between 24 and 48 h after exposure to h-IAPP. In contrast, the addition to dispersed islet cells of matured h-IAPP containing large amyloid deposits of organized fibrils was seldom associated with vesicle-like structures or features of cell death, even though the cells were often encased in the larger amyloid deposits. Based on these observations, we hypothesized that h-IAPP cytotoxicity is mediated by membrane damage induced by early h-IAPP aggregates. Consistent with this hypothesis, application of freshly dissolved h-IAPP to voltage-clamped planar bilayer membranes (a cell-free in vitro system) also caused membrane instability manifested as a marked increase in conductance, increased membrane electrical noise, and accelerated membrane breakage, effects that were absent using matured h-IAPP or rat IAPP solutions. Light-scattering techniques showed that membrane toxicity corresponded to h-IAPP aggregates containing ~25–6,000 IAPP molecules, an intermediate-sized amyloid particle that we term intermediate-sized toxic amyloid particles (ISTAPs). We conclude that freshly dissolved h-IAPP is cytotoxic and that this cytotoxicity is mediated through an interaction of ISTAPs with cellular membranes. Once ISTAPs mature into amyloid deposits comprising >10^6 molecules, the capacity of h-IAPP to cause membrane instability and islet cell death is significantly reduced or abolished. These data may have implications for the mechanism of cell death in other diseases characterized by local amyloid formation (such as Alzheimer's disease). ***Diabetes*** **48:491–498, 1999**

NIDDM is characterized by β-cell loss associated with the appearance of islet amyloid (1–4) derived from islet amyloid polypeptide (IAPP) (5,6). IAPP is a 37–amino acid protein that is highly conserved between species apart from amino acid residues 20–29, which show marked species divergence (7). This is also the region that confers amyloidogenic properties on the protein. Specifically, in any given species, if the motif arginine-isoleucine-leucine-serine-serine or similar is present (as in humans and cats) the peptide is amyloidogenic (8) and the species concerned is vulnerable to islet amyloid formation in NIDDM. In contrast, in rats and mice, this region of IAPP is not amyloidogenic (8), and these species do not spontaneously develop NIDDM characterized by islet amyloid. These observations imply that IAPP in the fibrillar form found in amyloid deposits may have a toxic effect within the islet. Several lines of evidence have recently emerged in support of the hypothesis that IAPP in an aggregated β-sheet (amyloid) form is cytotoxic.

Overexpression of human (h)-IAPP in COS cells led to intracellular h-IAPP amyloid aggregates and cell death, but this effect was not observed with comparable expression rates of rat (r)-IAPP (9). Also, application of h-IAPP to dispersed β-cells (and COS cells) led to local h-IAPP aggregates and cell destruction, an effect not observed with r-IAPP (10), although other reports have not observed cytotoxicity with h-IAPP (11). Recent studies with mice transgenic for h-IAPP have revealed a diabetic phenotype associated with the deposition of the h-IAPP in amyloid (12–15). In a prospective study of h-IAPP transgenic mice, we observed active β-cell destruction during the period of onset of diabetes in relation to the presence of small intracellular aggregates of h-IAPP, which were associated with local membrane abnormalities (13). We previously observed a similar relationship between abnormal membranes and intracellular IAPP aggregates in human insulinoma cells (16) and hypothesized that amyloid particles intermediate in size between h-IAPP monomers and the very large extracellular amyloid deposits visible by light microscopy—that is, the intermediate-sized amyloid particles—may be the most toxic form of aggregated IAPP. Additional evidence that h-IAPP aggregates may cause cell damage by their interactions with cell membranes was provided by the studies of Mirzabekov et al. (17), who showed that application of fresh solutions of h-IAPP (but not r-IAPP) to pla-

From the Departments of Medical Sciences (J.J., S.M., P.C.B.) and Pathology (D.H.) and the Membrane Biology Group (R.H.A., P.C.B.), University of Edinburgh, Edinburgh, Scotland, U.K.

Address correspondence and reprint requests to Peter C. Butler, MD, Department of Medical Sciences, Diabetic Medicine Section, The University of Edinburgh, Western General Hospital, Edinburgh EH4 2XU, Scotland. E-mail: p.butler@ed.ac.uk.

Received for publication 24 March 1998 and accepted in revised form 23 November 1998.

HBSS, Hanks' balanced salt solution; h-IAPP, human IAPP; IAPP, islet amyloid polypeptide; ISTAP, intermediate-sized toxic amyloid particle; LSM, laser scanning microscopy; r-IAPP, rat IAPP; TEM, transmission electron microscopy.

nar bilayers increased membrane conductance, apparently through induction of pores within the membranes.

In the present study, we addressed the following questions. *1*) Does the cytotoxicity of h-IAPP depend on the size of the h-IAPP aggregates? The application to cells of freshly prepared h-IAPP solutions containing intermediate-sized amyloid particles to dispersed mouse islet cells caused extensive membrane changes and was more cytotoxic than addition of matured h-IAPP solutions containing very large h-IAPP aggregates; we refer to these intermediate-sized particles as ISTAPs (intermediate-sized toxic amyloid particles). *2*) What is the time course and mechanism of cytotoxicity induced by ISTAPs in human islet cells? *3*) Do ISTAPs mediate their effect by disrupting cell membranes? This hypothesis was tested directly using planar bilayer membranes. *4*) What is the approximate size range of ISTAPs? Size was measured by relating the time course of particle growth (using standard light-scattering techniques) to quantifiable toxic effects observed on planar bilayers.

RESEARCH DESIGN AND METHODS

Mouse islet cell toxicity experiments

Islet isolation, culture, and monolayer preparation. Pancreatic islets were isolated from Friend virus B-type (FVB) mice at least 10 weeks old. The pancreas was perfused with 1.1 mg/ml collagenase (Type XI; Sigma, St. Louis, MO) in Hanks' balanced salt solution (HBSS) (Sigma) injected via the bile duct, using a 27- or 30-gauge needle and a syringe. The pancreas was digested for 16 min at 37°C. Islets were transferred to HBSS and concentrated on a Dextran gradient in HBSS. Islets were picked by hand and cultured in CMRL-1066 (Gibco, Rockville, MD) containing 5.5 or 16.6 mmol/l glucose, 10% (vol/vol) fetal calf serum (Hyclone Laboratories, Logan, UT), 2 mmol/l L-glutamine, 100 U/ml penicillin, and 100 mg/l streptomycin (Sigma) (18) at 37°C in humidified air containing 5% CO_2. The islet isolation procedure yielded islets in which most peripheral cells were β-cells, as previously described by El-Naggar et al. (19). h-IAPP added to islets in culture under these conditions will therefore encounter predominantly β-cells. To obtain an islet cell suspension, islets were trypsinized for 10 min at 37°C 1–3 days after isolation (10). The cells were then cultured using the medium and conditions described above.

Preparation of IAPP solutions. h-IAPP and r-IAPP were synthesized and purified by high-performance liquid chromatography in the Protein Core Facility of the Mayo Clinic, Rochester, MN. Peptide integrity was confirmed by amino acid analysis and plasma desorption time of flight mass spectrometry. To prepare mature h-IAPP in amyloid form, lyophilized h-IAPP was dissolved in water (for cell experiments) or buffer (for membrane experiments) at a concentration of 350 µmol/l. This h-IAPP stock solution was stored at 20°C for 7 days before application to cells or membranes. Freshly dissolved h-IAPP was prepared exactly as above but applied to islets or cells within 5 min of being dissolved.

Characterization of IAPP solutions. Samples of the h-IAPP solutions were examined before addition to cells or islets by use of both electron microscopy and a recently reported thioflavin-based assay (20). Samples of the cell or islet culture medium were collected and examined by electron microscopy shortly after addition of h-IAPP to the medium and also at the end of the culture period. For transmission electron microscopy (TEM), samples were prepared by the negative staining technique described by Betsholtz et al. (7). Amyloid fibrils were not observed by electron microscopy in either freshly prepared h-IAPP solutions or medium sampled from cells or islets after the addition of the freshly prepared h-IAPP solution. Amyloid fibrils were observed in the matured h-IAPP solutions and in medium sampled from cells or islets to which the matured h-IAPP solution had been added. The thioflavin-based assay confirmed these results in the freshly prepared versus matured h-IAPP solutions. We thus confirmed that matured h-IAPP solutions contained extensive amyloid fibrils in comparison with freshly dissolved h-IAPP.

Cytotoxicity protocols. To determine the effects of freshly prepared h-IAPP versus matured h-IAPP solutions on intact mouse islets or dispersed mouse islet cells, aliquots of these solutions were added to cell or islet cultures. Seven islet isolations (~650 islets from 4 mice per isolation) were performed; after overnight culture, the islets were divided into 3 comparable islet suspensions to which we added carrier solution only (control), freshly prepared h-IAPP solution, or matured h-IAPP solution. After addition of h-IAPP, the islet suspension was shaken thoroughly for 5 min to disperse the polypeptide throughout the islet suspension. The islets were then incubated at 37°C for 24 h. The effect of fresh versus matured h-IAPP solutions was then assessed by methods described below. Examination of the effects of h-IAPP aggregates added to intact islets may be confounded by penetration of the aggregates into the islet. To overcome this limitation, we also examined the effects of h-IAPP on the viability of dispersed islet cells by performing experiments similar to those described above for intact islets, but using dispersed islet cells. Six islet isolations (~650 islets from 4 mice per isolation) were used to obtain dispersed islet cell preparations (see above), which were divided into 3 aliquots and exposed to freshly prepared h-IAPP, matured h-IAPP, or carrier (control) and cultured for a further 24 h before assessment of cell viability. Both h-IAPP solutions were added to islet or islet cell suspensions to a final concentration of 40 µmol/l.

Assessment of h-IAPP effects. The effects of freshly prepared h-IAPP versus matured h-IAPP on intact islets were assessed by four methods: *1*) we counted the number of islets before and after exposure to h-IAPP or control solutions; *2*) we determined cell viability using confocal laser scanning microscopy (LSM); *3*) we measured islet size by light microscopy and image analysis; and *4*) we examined the islets with TEM. Numbers of islets were counted using an inverted microscope. LSM was performed by use of a Carl Zeiss LSM310 confocal microscope equipped with an argon/krypton laser with excitation lines at 488 and 568 nm. Green emission is taken between 515 and 545 nm, red emission >590 nm. In intact islets, only the two most peripheral cell layers could be studied, due to limited penetration of the laser. Preparation of islets for LSM involved the addition of 0.005% (wt/vol) propidium iodide (21,22) in phosphate-buffered saline containing 15 mg/l acridine orange (23) to an equal volume of islet suspension. Briefly, when such a preparation is examined by LSM, a red nucleus is observed in dead cells and a green nucleus in viable cells. Cell viability was calculated as the number of cells with a green nucleus divided by the total number of cells with green and red nuclei. Islet size was measured using morphometric analysis. Thick sections (0.5 µm) of Spurr resin–embedded samples were attached to light microscope slides and stained with toluidine blue. Islet area was determined using an automated image analysis system (Image-1 system; Universal Imaging, West Chester, PA) as previously reported (24). For TEM, islets were fixed in Trump's fixative (25) at 4°C, rinsed in 0.1 mol/l phosphate buffer, postfixed 1 h in 1% (wt/vol) OsO_4 in phosphate buffer, 30 min block-stained in 2% (wt/vol) uranyl acetate, dehydrated in a graded ethanol series, transferred to propylene oxide, and embedded in Spurr resin (26). Thin sections on nickel grids were immunogold-labeled for IAPP (13). After drying, sections were stained with lead citrate for 5 min and observed with a Jeol 1200 (Jeol, Peabody, MA). Individual IAPP immunoreactive fibrils were <12 nm in diameter, the size of the immunogold particles. The effects of exposing dispersed islet cells to freshly prepared h-IAPP versus matured h-IAPP solutions or carrier (control) were determined by LSM and by electron microscopy as described for intact islets.

Time course and mechanism of h-IAPP cytotoxicity in human islet cells (n = 4). From the electron microscopic appearance of dispersed mouse islet cells exposed for 24 h to fresh h-IAPP, we noted cell membrane disruption in cells but the percentage of cells killed was relatively small. To extend these observations, we therefore performed a similar experiment using dispersed human islet cells exposed to fresh h-IAPP, mature h-IAPP, r-IAPP, and control solution for 48 h to determine *1*) whether fresh versus mature h-IAPP solutions are cytotoxic to human as well as rodent islet cells; *2*) whether the relatively high percentage of islet cells apparently injured 24 h after exposure to fresh h-IAPP subsequently die; and *3*) whether the mechanism of this death is by apoptosis or necrosis or both.

Isolation, culture, and monolayer preparation of human islets. Islets were obtained from the University of Leicester Department of Surgery by collagenase digestion. Approximately 5,000 human islets were obtained and cultured in RPMI 1640 at 5.5 mmol/l glucose for 4 days before dispersal by gently shaking in Ca^{2+}-free solution. The dispersed human islet cells were divided into aliquots onto plastic chamber slides (chamber slide culture chambers, Lab-Tek; Nunc, Naperville, IL). After 72 h of culture in RPMI 1640, freshly prepared h-IAPP, matured solution of h-IAPP, freshly dissolved r-IAPP, or an equivalent volume of water was added to the culture medium as described above.

Assessment of cytotoxicity. Dispersed islet cells were examined by phase-contrast light microscopy in situ on the chamber slide and photographed before and 24 and 48 h after addition of IAPP. At 48 h after addition of IAPP, the cells were fixed in situ on the slide with methanol/acetic acid and nuclei were stained with hematoxylin for subsequent examination. The medium in each chamber was aspirated and centrifuged, and the pellet was fixed for subsequent examination for number of cells and cell viability using acridine orange staining and visualization under ultraviolet light. At 48 h after exposure of cells to IAPP, representative fields from each chamber were digitally photographed (magnification 200×) and the images stored for subsequent analysis. Analysis included counting the number of viable cells per microscopy field and assessing the number of the cells that were either apoptotic or necrotic in the same field. Apoptotic cells were identified by morphologic fragmentation of the nucleus. While this

method does not detect all apoptotic cells, it is reliable and reproducible and has been used previously (27). Necrosis was scored where there was dissolution of the nucleus and obvious disruption of plasma membrane. With acridine orange staining, apoptosis was seen as condensed, bright green fluorescent nuclear staining, whereas necrosis showed yellow-green ill-defined staining, indicating denaturation of double-stranded DNA.

Effect of h-IAPP on planar bilayer membranes. Bilayer recording was carried out using the methods and apparatus described by Williams (28). Briefly, a styrene copolymer cup with a 0.6-ml inner chamber containing a magnetic stirbar was nested in a 0.6-ml Perspex outer chamber, and both chambers were filled with 10 mmol/l KCl containing 20 mmol/l Tris-HCl (pH 7.4). These relatively low-salt conditions were chosen for the bilayer experiments to optimize IAPP–membrane interaction (17). Bilayers were cast from equimolar palmitoyl-oleoyl phosphatidylserine and palmitoyl-oleoyl phosphatidylethanolamine (Avanti Polar Lipids, Alabaster, AL) suspended in *n*-decane (Aldrich, Gillingham, Dorset, U.K.; final concentration 30 mg/ml) by drawing ~1 µl of the mixture across a 0.3-mm hole separating the two solution-filled chambers. The cup (*cis*) chamber was voltage-clamped relative to the outer (*trans*) chamber, which was grounded, using a Biologic RK-300 patch-clamp amplifier. Transmembrane currents were low-pass filtered at 0.3–10 kHz (–3 dB, 8-pole Bessel-type response) and recorded. Membrane capacitance was measured by differentiating a precalibrated triangle wave command voltage. The membranes, which thinned spontaneously over 2–3 min to give a central bilayer surrounded by a thin "annulus" or "torus" of the original decane lipid suspension, were routinely monitored for the first 14 min to ensure compliance with the following criteria: minimum capacitance 250 pF, maximum conductance 5 pS, maximum bilayer noise 2 pA (peak-to-peak, filtered at 0.3 kHz). Membranes that failed to meet these criteria were not used, and membranes were also discarded if they showed evidence of instability, such as variations in conductance. IAPP (10 µmol/l) was added directly to the *cis* chamber, which was voltage-clamped at +50 mV, and stirred in for exactly 1 min. The IAPP was freshly dissolved h-IAPP (applied to membranes within 3 h), fibrillar h-IAPP dissolved 1 week before the experiment, or r-IAPP, all prepared as 350 µmol/l stock solutions in 10 mmol/l KCl containing 20 mmol/l Tris-HCl (pH 7.4) in silinised tubes. The membrane potential was maintained at +50 mV between measurements, and at timed intervals, membrane currents were recorded at +50 and –50 mV and analyzed later to determine the membrane chord conductance. Recordings were made at intervals up to 80 min, or until the bilayer broke. Analysis was carried out using pClamp6 software (Axon Instruments, Foster City, CA).

Assessment of size of toxic amyloid particles. The size distribution of h-IAPP particles in 350 µmol/l solution was determined by standard light-scattering techniques (29) using a DynaPro-801TC instrument (Protein Solutions, Charlottesville, VA).

Statistical analysis. Comparisons of reduction in number of islets, viability of cells situated in the periphery of islets, mean islet area, and bilayer membrane capacitance were made by analysis of variance. Dispersed islet cell viability was calculated relative to the viability in control cultures, and treatment with freshly dissolved h-IAPP was compared with fibrillar h-IAPP treatment using a nonpaired, two-tailed Student's t test. Membrane conductance measurements were subjected to multiple regression analysis. For fresh h-IAPP additions, where membrane breakage was accelerated, statistical analysis was restricted to the time points for which at least 50% of the membranes remained unbroken. For application of freshly dissolved or fibrillar h-IAPP after pre-exposure to fibrillar h-IAPP, analysis of membrane conductance was restricted to data obtained after the second application. Membrane lifetimes were subjected to multiple regression analysis. Data are presented as means ± SE unless stated otherwise.

RESULTS

Mouse islet cell cytotoxicity

h-IAPP applied to intact islets. The percentage survival of viable intact islets by the end of culture was no different after exposure to freshly prepared versus matured h-IAPP solutions and controls (control 90 ± 14, matured 90 ± 12, and fresh 91 ± 15%, mean ± standard deviation, $P = 0.96$).

After an overnight culture of intact islets, some cell death occurred with each treatment, as indicated by LSM. The number of dead cells observed after treatment with fresh or mature h-IAPP was not increased (viability of the outer two cell layers: control 90 ± 2.3, matured 89 ± 2.0, and fresh 80 ± 6.4%, $P = 0.24$).

Examination of islets exposed to fresh versus matured h-IAPP solutions revealed a comparable mean islet cross-sec-

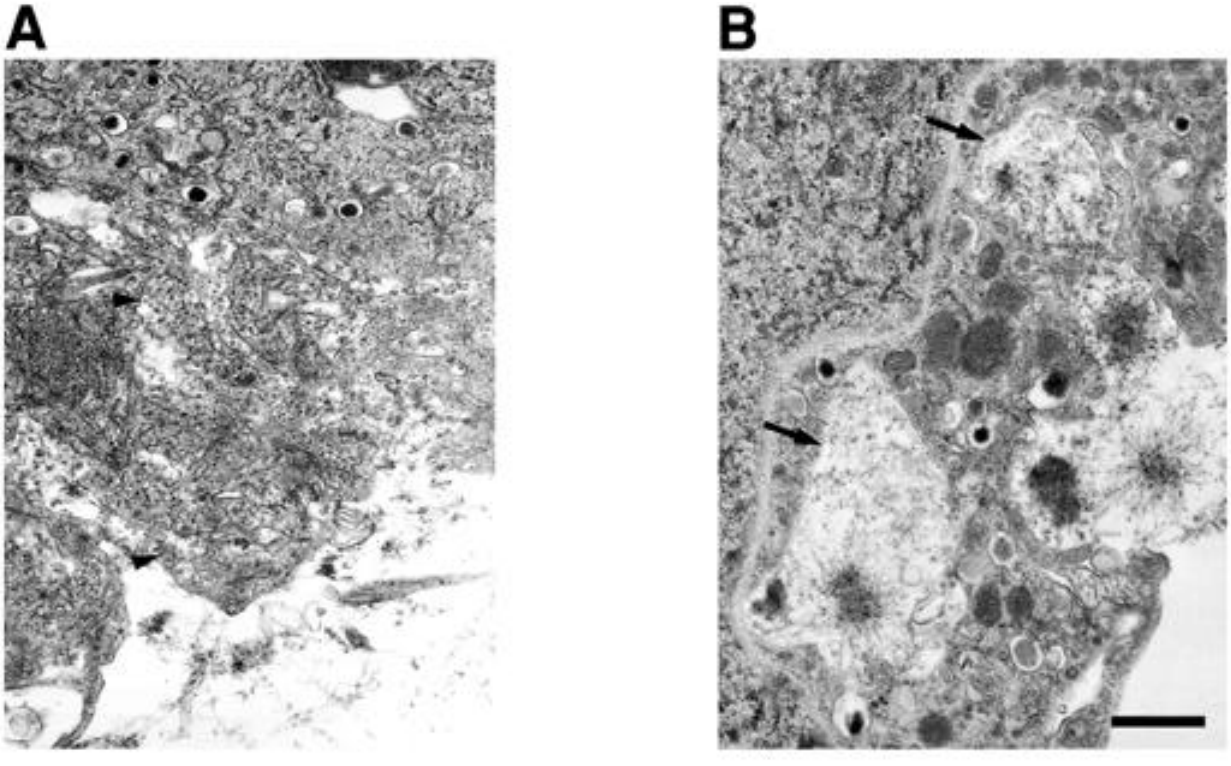

FIG. 1. Representative electron micrographs (with immunogold-labeled IAPP) showing peripheral cells of mouse islets exposed to freshly dissolved h-IAPP (*A*) or preformed h-IAPP–derived amyloid (*B*). Cells exposed to freshly dissolved IAPP show extensive intermingling of IAPP labeling and cellular membranes. Membranes form numerous vesicle-like structures (arrowheads), and the morphology is grossly abnormal. In contrast, cells exposed to preformed amyloid (*A*) are often coated with mature amyloid deposits which occasionally penetrate deeply within the cell, but the projections are still membrane-bound (arrows). The overall cell morphology is more normal than in peripheral islet cells exposed to freshly dissolved h-IAPP. Scale bar = 0.5 µm.

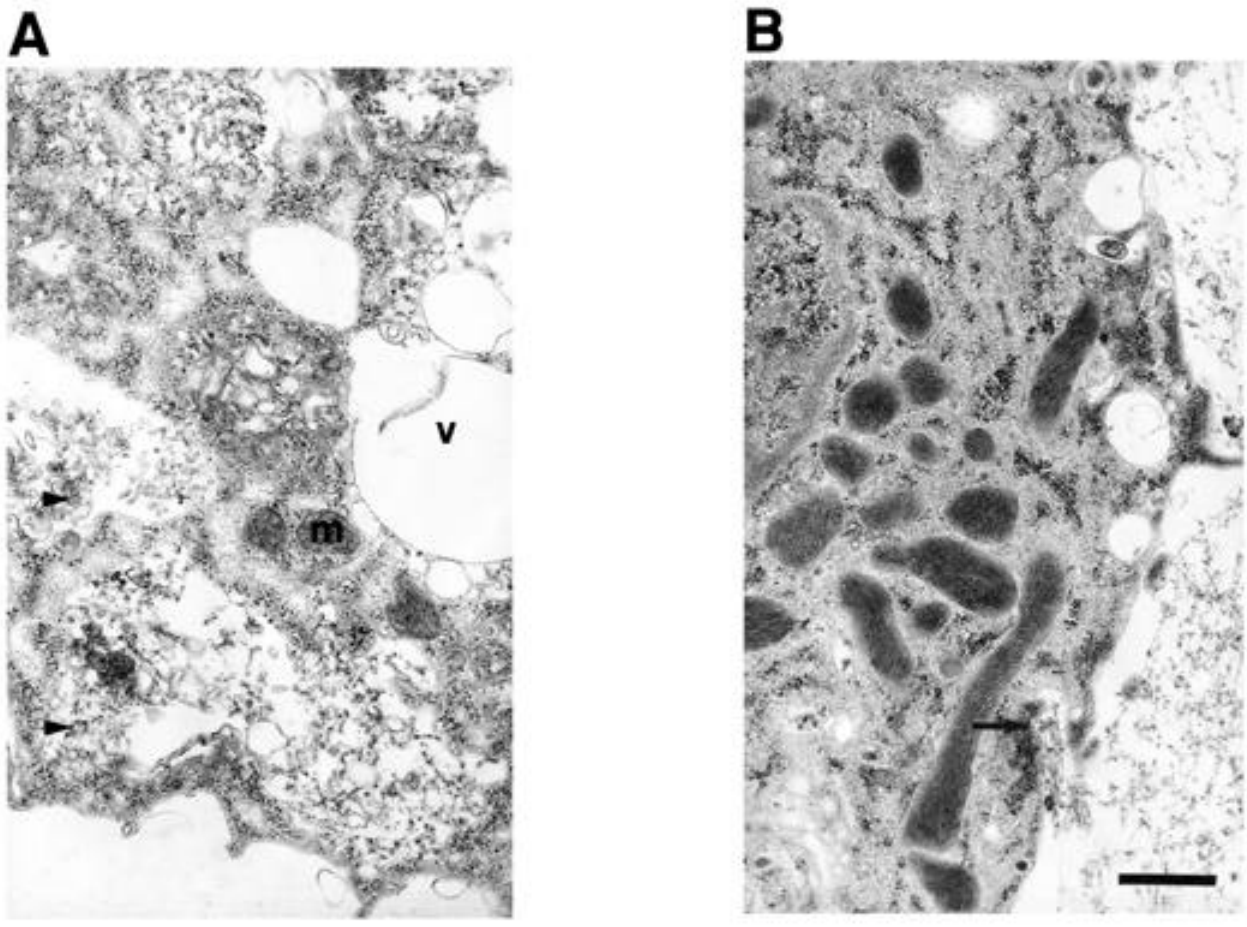

FIG. 2. Representative electron micrographs (with immunogold-labeled IAPP) of dispersed mouse islet cells after exposure to freshly dissolved h-IAPP (*A*) or h-IAPP–derived amyloid (*B*). Cells treated with freshly dissolved h-IAPP show abnormal vesiculation associated with IAPP labeling (arrowheads), a high degree of vacuolization (v), and swollen mitochondria (m). In contrast, cells exposed to preformed amyloid are often coated in IAPP-immunoreactive amyloid, which occasionally penetrates the cells (arrow), but they do not show extensive vesicle formation, abnormal mitochondria, or vacuolization. Scale bar = 0.5 µm.

tional area compared with controls (control 10,470 ± 1,800; matured 11,580 ± 2,500; and fresh 8,060 ± 1,540 µm^2, $P = 0.46$).

In untreated islets, no IAPP-immunoreactive deposits were observed by electron microscopy. After application of fresh or mature h-IAPP to islets, immunoelectron microscopy showed amorphous and fibrillar IAPP immunoreactive material present in the medium, in close association with islets, and in the periphery but not in the center of islets. Some of the peripheral cells of islets treated with freshly dissolved h-IAPP showed abnormal morphology, with an intermingling of cellular membranes and IAPP-immunoreactive deposits (Fig. 1*A*). Similar abnormalities were observed with dispersed islet cells treated with freshly dissolved h-IAPP (described in more detail below). After treatment with fibrillar h-IAPP, some cells were heavily invaded by IAPP fibrils, but the presence of IAPP fibrils was not associated with cell degeneration or abnormal morphology (Fig. 1*B*). Matured h-IAPP, surrounded by the indented cell membrane, penetrated cells to reach as far as the nucleus without signs of degeneration (Fig. 1*B*). Taken together, these observations in intact islets suggested that freshly prepared h-IAPP was causing toxicity to the outer rim of cells of the islet, but the toxicity was difficult to quantify in the intact islet, where only a small fraction of cells is exposed. We therefore proceeded to studies with dispersed islet cells.

h-IAPP applied to dispersed mouse islet cells (24 h). Fresh h-IAPP showed evidence of cytotoxicity when applied to dispersed cells, but there was no reduction in cell viability as assessed by LSM when isolated islet cells were treated with fibrillar h-IAPP (viability relative to control treatments: fibrillar 104 ± 4 vs. fresh 88 ± 6%, $n = 6$, $P < 0.05$).

As assessed by electron microscopy, after treatment with either fresh or matured solutions, h-IAPP–immunoreactive deposits were present surrounding the cells. After the addition of matured h-IAPP, these deposits were only present in clearly defined fibrillar form, but after the addition of freshly dissolved h-IAPP, amorphous deposits of h-IAPP were also present. The most striking effect of freshly dissolved h-IAPP was the appearance of a markedly abnormal mass of small vesicle-like structures packed closely together (Fig. 2*A*). This appearance was only present in association with amorphous IAPP immunoreactivity, and therefore only present in cultures exposed to fresh h-IAPP; when it was present, the affected cells were vacuolated and undergoing degeneration (Fig. 2*A*). In contrast, β-cells remained healthy after treatment with matured h-IAPP, even if the cells were surrounded, and occasionally penetrated, by fibrillar h-IAPP (Fig. 2*B*). The relatively high proportion of cells with abnormal cell membranes 24 h after exposure to freshly prepared h-IAPP, compared

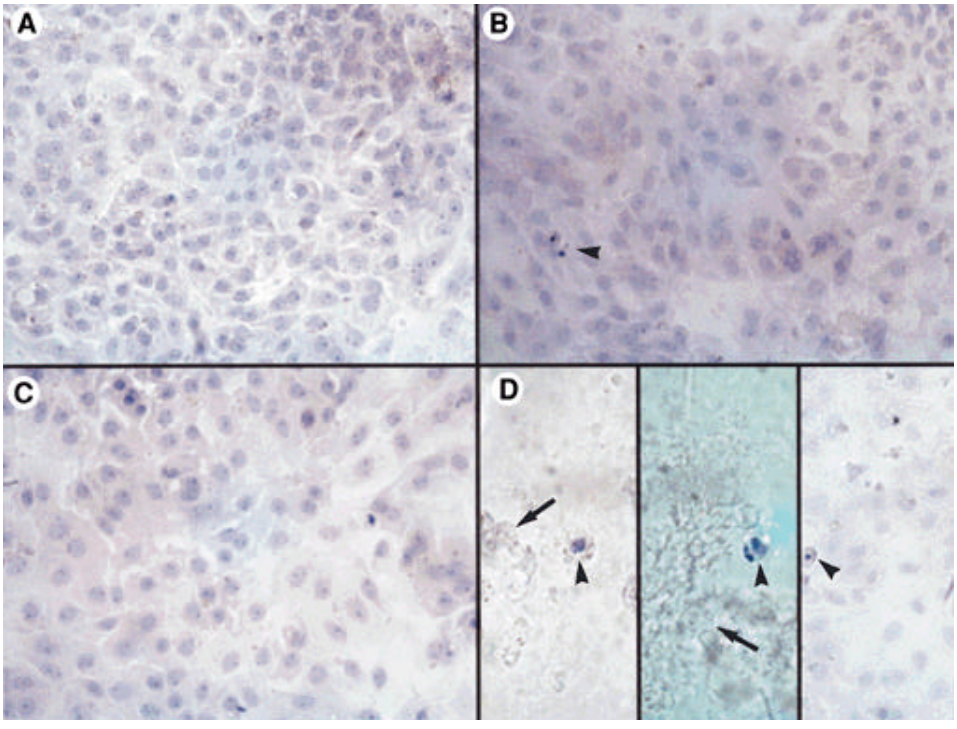

FIG. 3. Human islet cells. *A*: Monolayer of flattened β-cells after 48 h in culture. *B*: After treatment with r-IAPP, cultures were indistinguishable from controls, with only occasional apoptotic cells (arrowhead). *C*: Similar findings were seen with mature h-IAPP. *D*: With fresh h-IAPP after 48 h, there were clearly identified apoptotic cells (arrowheads) and anuclear necrotic debris (arrows) as well. Some viable cells remained, but they were sometimes rounded up and had less distinct nucleoli.

with the ~15% of cells killed, suggested that cell destruction as a result of this treatment may continue after 24 h. We therefore proceeded to studies for 48 h and, as they had recently become available, extended the observations to human islets.

Time course and mechanism of h-IAPP toxicity in human islet cells. The density of dispersed human islet cells in the different chambers was comparable before addition of IAPP. After addition of IAPP (24 h), there were no discernable differences between the cells exposed to mature h-IAPP, r-IAPP, or control; the cells all showed flattening and a regular shape. In contrast, cells exposed to freshly dissolved h-IAPP for 24 h were less regular in appearance, and occasional necrotic cells and cellular debris were present. After 48 h, this distinction was more marked (Fig. 3*A*–*C* vs. *D*). More than 50% reduction ($P < 0.01$) in cell viability was observed in cells exposed to freshly dissolved h-IAPP ($P < 0.001$) compared with mature h-IAPP, r-IAPP, or control, which were again indistinguishable from one another. Islet cells from the latter showed occasional mitosis and distinct cytoplasmic organelles. Some of the remaining cells exposed to freshly dissolved h-IAPP were morphologically normal. The percentages of cells identifiable at 48 h after exposure to IAPP or control that were apoptotic: fresh h-IAPP, 14%; mature h-IAPP, 8%; control, 0%; r-IAPP, 0% ($P < 0.01$); and necrotic: fresh h-IAPP, ≥12%; mature h-IAPP, 0%; control, 0%; r-IAPP, 0% ($P < 0.01$).

Only very occasional apoptotic and necrotic cells were visualized by acridine orange staining in supernatants.

H-IAPP applied to planar bilayer membranes. The capacitance of a bilayer or cell membrane is directly proportional to its area. The mean initial bilayer capacitance was 275 ± 13 pF ($n = 30$), consistent with a diameter of ~0.3 mm (30). The values measured 5 min after adding freshly dissolved h-IAPP, fibrillar h-IAPP dissolved 7 days before the experiment, or r-IAPP were not significantly different. Addition of freshly dissolved h-IAPP, however, did result in rapid membrane destabilization, manifested as increased membrane electrical noise (Fig. 4*A*), a significant increase in conductance ($P < 0.05$ within 5 min; Fig. 4*B*), and accelerated membrane breakage ($P < 0.05$; Fig. 4*C*). The leak (increased conductance) induced by freshly dissolved h-IAPP was usually asymmetric or rectifying, as observed by Mirzabekov et al. (17), but the direction of rectification was not constant from experiment to experiment. We therefore measured the maximum conductance, corresponding to the maximum chord conductance at either +50 or –50 mV, as appropriate.

These changes were seen regardless of the prior presence of fibrillar h-IAPP, which by itself had little or no effect at 10 and 20 µmol/l (Fig. 4). This finding is consistent with the hypothesis that freshly dissolved but not matured solutions of h-IAPP cause membrane disruption. In addition, application of freshly dissolved h-IAPP increased the membrane conductance more rapidly than application of r-IAPP ($P < 0.005$; Fig. 4*B*), confirming that the mechanism of membrane disruption by freshly dissolved h-IAPP solutions is dependent on the presence of β-sheets of h-IAPP. We noticed that occasionally (3 of 17 additions), addition of freshly dissolved h-IAPP had little or no effect over the time-course of an experiment, possibly because the hydrophobic peptide was sequestered by the lipid annulus and failed to reach the bilayer itself despite vigorous stirring. Nevertheless, these data have been included in Fig. 4*B*.

Sizing of toxic amyloid particles using light scattering. The change of IAPP particle size during the first 3 h after the addition of lyophilized peptide to solvent is shown for r- and h-IAPP in Fig. 5. Freshly prepared solutions of r-IAPP "dissolved" completely as time progressed, achieving a size consistent with monomeric r-IAPP by 120 min. In contrast, a freshly prepared solution of h-IAPP progressively increased in

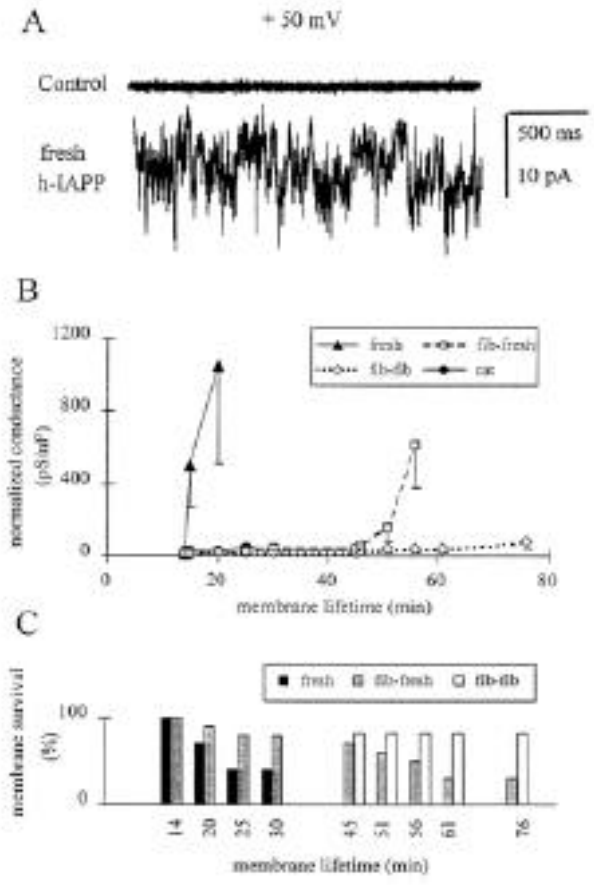

FIG. 4. IAPP applied to planar bilayer membranes. *A*: Control recording and the same membrane 5 min after adding 10 µmol/l freshly dissolved h-IAPP to the *cis* chamber. Note membrane instability and increase in membrane electrical noise. Filtered at 0.3 kHz. *B*: Membrane conductance normalized for capacitance (relative area) after treatment with freshly dissolved h-IAPP (fresh), fibrillar h-IAPP followed by freshly dissolved h-IAPP (fib-fresh), fibrillar h-IAPP followed by fibrillar h-IAPP (fib-fib), or r-IAPP (rat). Note the large increase in conductance after adding freshly dissolved h-IAPP to untreated membranes ($P < 0.05$ fresh vs. fib-fresh), and in membranes incubated with fibrillar h-IAPP for 30 min ($P < 0.005$ fib-fresh vs. fib-fib). *C*: Membrane survival is reduced after exposure to freshly dissolved h-IAPP compared with fibrillar h-IAPP (up to 30 min; $P < 0.05$ fresh vs. fib-fresh). When added to fibrillar h-IAPP, freshly dissolved h-IAPP added to fibrillar h-IAPP reduces membrane survival, while fibrillar h-IAPP does not ($P < 0.005$ fib-fresh vs. fib-fib).

size throughout the period of observation. The actual molecular weight of nonglobular proteins (such as amyloid particles) can only be approximated by this technique because the time-resolved tumbling of asymmetric particles in solution is mathematically highly complex compared with spherical particles, but it appears that the h-IAPP particles corresponding to those that cause planar bilayer membrane disruption (0- to 180-min solutions) contain aggregates of h-IAPP of intermediate size (initially between 25 and 500 monomers and growing to 2,000–6,000 h-IAPP monomers per particle). They were clearly not monomers, and certainly not the very large particles present in matured h-IAPP (>10^6 h-IAPP molecules per particle). We thus defined these toxic particles as ISTAPs.

DISCUSSION

In the present study, we sought to determine the relative cytotoxicity on islet cells of freshly dissolved h-IAPP containing ISTAPs versus much larger h-IAPP fibrils. We report that freshly dissolved h-IAPP was cytotoxic to dispersed islet cells, and that this cytotoxicity is characterized by dramatic disruption and vesiculation of cell membranes. Disruption of cell membranes was the most obvious feature 24 h after exposure to ISTAPs, with both necrotic and apoptotic cells seen at 48 h. Consistent with the ultrastructural observation that fresh h-IAPP disrupted cell membranes, we report that in an in vitro system, freshly dissolved h-IAPP causes membrane destabilization, an effect not observed with nonfibrillar r-IAPP or matured h-IAPP solutions containing large amyloid deposits (>10^6 monomers). To characterize the nature of the toxic particles of h-IAPP in relation to membrane toxicity, we used standard light-scattering measurements to establish the approximate size of the toxic h-IAPP particles. These particles were at least two orders of magnitude smaller than mature amyloid fibrils, and we defined them as intermediate-sized toxic amyloid particles (ISTAPs). We propose that the toxicity induced by such particles may be of general importance in the mechanism of amyloid-associated cell destruction, for example in Alzheimer's disease.

Using the same concentration of h-IAPP as in the present study, Lorenzo et al. (10) reported that h-IAPP was cytotoxic to islets and dispersed islet cells and that the cytotoxicity was associated with the presence of IAPP aggregates on the cell surface. In contrast, r-IAPP did not cause cell death, implying that the β-pleated sheet structure present in amyloid is required for the observed cytotoxicity. Of note, in those experiments, Lorenzo et al. added freshly prepared solutions of h-IAPP to the cells (10). In contrast, Clark et al. (11) reported that addition of matured h-IAPP–derived fibrils to islets was not cytotoxic. Recently, however, the same group reported that h-IAPP causes cytotoxicity to β-TC cells with a similar time course to that shown here. The source of IAPP may be important in cytotoxicity (31). One possible explanation for these discrepant data is that h-IAPP cytotoxicity, like that of β protein (32), decreases with maturity of the h-IAPP solution. Amyloid is formed by polymerization of a monomeric

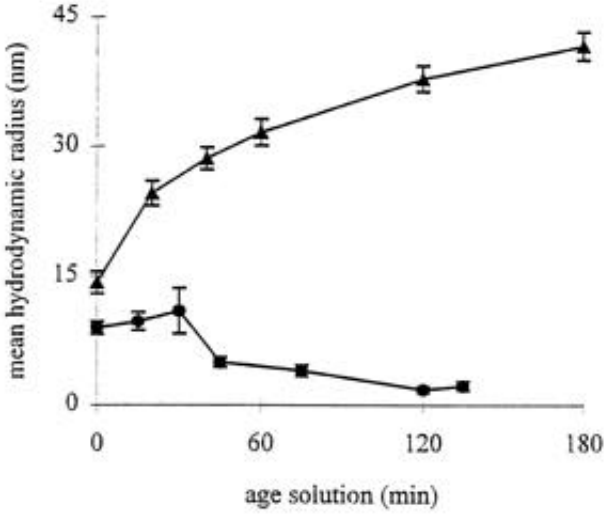

FIG. 5. Hydrodynamic radius, a measure of particle size, of representative 350-µmol/l h-IAPP and r-IAPP solutions freshly prepared at 0 min. Note the increase in particle size over time for the h-IAPP particles (▲), while r-IAPP particles (●) do not grow. Each data point is the mean ± SD of 20 measurements.

protein or peptide with a tendency to form a β-sheet fibril structure under appropriate conditions. The growth of amyloid fibrils progresses with time from monomers through intermediate-sized fibrillar structures (visible by electron microscopy but not light microscopy) toward very large amyloid deposits (visible by light microscopy) that comprise $>10^6$ monomers. If h-IAPP cytotoxicity does decline with the maturity of the h-IAPP solution, it would appear *1*) that cytotoxicity requires aggregates of the protein in β-sheet structure (hence toxicity with h-IAPP but not r-IAPP), but *2*) that these aggregates lose their toxicity when they grow beyond a certain size. Our data strongly support this hypothesis, but provoke two questions: Why is freshly dissolved h-IAPP more cytotoxic than matured amyloid fibrils? By what mechanism does freshly dissolved h-IAPP cause cytotoxicity?

Some insight into the second of these questions was provided by the intriguing studies of Mirzabekov et al. (17). Using artificial lipid bilayer membranes, they reported that human (but not rat) IAPP solutions markedly increased membrane conductance, possibly as a result of pore formation. The present studies reconfirm this work and extend it by revealing that freshly prepared but not matured h-IAPP solutions cause membrane instability, implying that the latter is a function of the size of the h-IAPP–derived amyloid particles. In the present study, we provide additional evidence in support of the hypothesis that h-IAPP cytotoxicity is mediated through disruption of cell membranes by reporting changes in the membranes of dispersed islet cells exposed to freshly dissolved h-IAPP solutions as examined by electron microscopy. These cells showed marked disruption of cell membranes, including the appearance of an abnormal mass of vesicle-like structures that were associated with small amorphous IAPP deposits in dead or dying cells. In contrast, cells exposed to matured h-IAPP solutions were often encased in and surrounded by mature amyloid fibrils (which occasionally penetrated cells), but the cells remained viable, with normal cell membranes. In particular, they were not disrupted into vesicle-like structures despite being directly adjacent to large amyloid deposits. If the mechanism of h-IAPP cytotoxicity is disruption of cell membrane stability by interaction of h-IAPP hydrophobic aggregates with the membranes, it is logical that this process will depend on the size (and hence maturity) of the h-IAPP aggregates. Once an h-IAPP aggregate becomes very large and the hydrophobic regions of h-IAPP are confined within the aggregate, it would lose its capacity to become interpolated within the membrane. Such a model, in which cytotoxicity depends on h-IAPP aggregate size, would be consistent with published observations in mice transgenic for h-IAPP.

Mice homozygous for a h-IAPP transgene developed diabetes spontaneously as a consequence of β-cell destruction (13). In those mice, cell destruction was associated with the presence of numerous small intracellular IAPP aggregates (apparent by electron but not light microscopy) in an amorphous form, similar to the h-IAPP deposits observed adjacent to islet cells undergoing marked membrane disruption in the present studies. In contrast, in the same mice, organized mature amyloid deposits (visible by electron microscopy) only became apparent some weeks after the period of maximal β-cell toxicity, implying at most a relatively minor role for these mature IAPP amyloid deposits in cell toxicity. These findings are consistent with the viability of dispersed islet cells exposed to mature amyloid in the present experiments. This disassociation between cell death and the appearance of the large extracellular amyloid deposits implies that the appearance of a precursor to the extracellular amyloid deposits may lead to cell death, after which it is released to the extracellular environment, where it would presumably be trapped on the vascular endothelium and grow as a secondary event. This model is also consistent with the observation that islet cell toxicity associated with islet amyloid appearance is confined to β-cells and not α- or δ-cells in both transgenic mouse models (13,14) and humans with NIDDM. If h-IAPP toxicity was mediated by the growing extracellular amyloid deposits, it would be expected to affect non–β-cells, as well, when they came into contact with it. Additional evidence against the cytotoxicity of mature amyloid deposits is the observation that healthy cells are bordered by large amyloid deposits in human insulinomas (16), islets of patients with NIDDM (33), and h-IAPP transgenic mouse islets in vivo (14) and cultured in vitro (34). We have suggested that h-IAPP cytotoxicity arises from intracellular aggregates of h-IAPP (9,12,13,16,24); how do the present data showing extracellularly applied h-IAPP relate to that model? We propose that the specific mechanism of h-IAPP toxicity is through membrane disruption. Of course, the vast majority of cell membrane is intracellular, and we have reported abnormalities of intracellular membrane structures in association with intracellular IAPP aggregates (9,12,13,16). We believe, therefore, that the finding that ISTAPs are cytotoxic through the specific mechanism of cell membrane disruption when applied extracellularly is consistent with the hypothesis that intracellular aggregates of ISTAPs lead to local intracellular membrane disruption and subsequent cell death.

In the present study, at 24 h, dead cells were uncommon; those that were present showed features of necrosis. Interestingly, as reported by Higham et al. (31), we observed in dispersed human islet cells that β-cell death occurred predominantly after 24-h exposure to h-IAPP, by both apoptosis and necrosis. Since apoptotic cells may undergo secondary necrosis, it is possible that we have overestimated the frequency of necrosis. The fact that an insult to the cell membrane caused by ISTAPs does not result in cell death until 48 h later is certainly consistent with the notion that there is a requirement for induction and expression of effector proteins. Consistent with these observations, Lorenzo et al. (10) reported that exposure of islets or islet cells to h-IAPP caused apoptosis. Cytotoxicity by β protein has also been reported to express itself by apoptosis (35) and necrosis (36). From the present studies, these discrepancies may be related to the rate and extent of cell damage inflicted by the amyloidogenic proteins in different experiments. In support of this conjecture, membrane damage caused by h-IAPP was directly proportional to the concentration applied to the membrane (17), and both h-IAPP and β protein toxicities are partly mediated by an oxidative mechanism (37). The production of intracellular peroxides after exposure of cells to β protein increases as a function of the β protein concentration (38), and cell death has been shown to be apoptotic or necrotic, depending on pro-oxidant levels (39).

In conclusion, we have carried out in vivo and in vitro experiments that support a new hypothesis relating IAPP to NIDDM. We confirm that h-IAPP is cytotoxic to dispersed mouse and human islet cells when applied in a freshly prepared solution. Under these conditions, the cells show abnormal membrane vesicle formation colocalized with deposits of

amorphous h-IAPP. In contrast, when preformed IAPP-derived amyloid is applied to the same cells, no cytotoxicity is detected. h-IAPP cytotoxicity thus appears to be mediated via membrane damage, but only when h-IAPP is in its nascent, nonfibrillar (or early fibril) physical state. Between 24 and 48 h after exposure to this damage, a high proportion (~50%) of islet cells undergo cell death through apoptosis or necrosis. These observations support the hypothesis that the mechanism of β-cell damage in NIDDM is the abnormal aggregation of a hydrophobic protein, IAPP, into a toxic polymer containing <10,000 monomers that disrupts local membranes. This novel mechanism may be important in other diseases characterized by cell death associated with local amyloid deposits comprising a hydrophobic protein produced by the vulnerable cells (such as cortical neurons in Alzheimer's disease). Measures to prevent this membrane damage may provide novel approaches to prevent or treat NIDDM.

ACKNOWLEDGMENTS

The work was supported by grants from the U.S. Public Health Service (DK-44341), Pfizer, the Mayo Foundation, the Wellcome Trust (grant numbers 049853 and 043420), the British Diabetic Association (grant to Leicester University Department of Surgery), and the University of Edinburgh. The human islets were provided by the University of Leicester Department of Surgery by Dr. Heather Clayton and Dr. Sue Swift.

The authors thank Karen Laakso for mouse islet isolation and Joyce Sackett and Susan Gossman for help with sectioning. We appreciate the constructive suggestions of Dr. Walter Soeller, Pfizer; Professor Malcolm Walkinshaw (Structural Biochemistry) at the University of Edinburgh; and Dr. Mark Dunne from the University of Sheffield.

REFERENCES

1. Westermark P: Quantitative studies of amyloid in the islets of Langerhans. *Ups J Med Sci* 77:91–94, 1972
2. Clark A, Wells CA, Buley ID, Cruickshank JK, Vanhegan RI, Matthews DR, Cooper GJ, Holman RR, Turner RC: Islet amyloid, increased A-cells, reduced B-cells and exocrine fibrosis: quantitative changes in the pancreas in type 2 diabetes. *Diabetes Res* 9:151–159, 1988
3. Johnson KH, O'Brien TD, Betsholtz C, Westermark P: Islet amyloid, islet-amyloid polypeptide, and diabetes mellitus. *N Engl J Med* 321:513–518, 1989
4. Johnson KH, O'Brien TD, Betsholtz C, Westermark P: Islet amyloid polypeptide: mechanisms of amyloidogenesis in the pancreatic islets and potential roles in diabetes mellitus. *Lab Invest* 66:522–535, 1992
5. Westermark P, Wernstedt C, Wilander E, Hayden DW, O'Brien TD, Johnson KH: Amyloid fibrils in human insulinoma and islets of Langerhans of the diabetic cat are derived from a neuropeptide-like protein also present in normal islet cells. *Proc Natl Acad Sci U S A* 84:3881–3885, 1987
6. Cooper GJS, Willis AC, Clark A, Turner RC, Sim RB, Reid KBM: Purification and characterization of a peptide from amyloid-rich pancreases of type 2 diabetic patients. *Proc Natl Acad Sci U S A* 84:8628–9632, 1987
7. Betsholtz C, Christmansson L, Engström U, Rorsman F, Svensson V, Johnson KH, Westermark P: Sequence divergence in a specific region of islet amyloid polypeptide (IAPP) explains differences in islet amyloid formation between species. *FEBS Lett* 251:261–264, 1989
8. Westermark P, Engström U, Johnson KH, Westermark GT, Betsholtz C: Islet amyloid polypeptide: pinpointing amino acid residues linked to amyloid fibril formation. *Proc Natl Acad Sci U S A* 87:5036–5040, 1990
9. O'Brien TD, Butler PC, Kreutter DK, Kane LA, Eberhardt NL: Human islet amyloid polypeptide expression in COS-1 cells. A model of intracellular amyloidogenesis. *Am J Pathol* 147:609–616, 1995
10. Lorenzo A, Razzaboni B, Weir GC, Yankner BA: Pancreatic islet cell toxicity of amylin associated with type-2 diabetes mellitus. *Nature* 368:756–760, 1994
11. Clark A, Badman MK, Lowndes SA, Morris JF: Aggregated human islet amyloid polypeptide is not cytotoxic to mouse islets *in vitro* (Abstract). *Diabetologia* 38 (Suppl. 1):A91, 1995
12. Couce M, Kane LA, O'Brien TD, Charlesworth J, Soeller W, McNeish J, Kreutter D, Roche P, Butler PC: Treatment with growth hormone and dexamethasone in mice transgenic for human islet amyloid polypeptide causes islet amyloidosis and β-cell dysfunction. *Diabetes* 45:1094–1101, 1996
13. Janson J, Soeller WC, Roche PC, Nelson RT, Torchia AJ, zKreutter DK, Butler PC: Spontaneous diabetes mellitus in transgenic mice expressing human islet amyloid polypeptide. *Proc Natl Acad Sci U S A* 93:7283–7288, 1996
14. Soeller WC, Janson J, Hart SE, Parker JC, Carty MD, Stevenson RW, Kreutter DK, Butler PC: Islet amyloid-associated diabetes mellitus in obese A^{vy}/a mice expressing human IAPP. *Diabetes* 47:743–750, 1998
15. Verchere CB, D'Alessio DA, Palmiter RD, Weir GC, Bonner-Weir S, Baskin DG, Kahn SE: Islet amyloid formation associated with hyperglycemia in transgenic mice with pancreatic β cell expression of human islet amyloid polypeptide. *Proc Natl Acad Sci U S A* 93:3492–3496, 1996
16. O'Brien TD, Butler AE, Roche PC, Johnson KH, Butler PC: Islet amyloid polypeptide in human insulinomas. *Diabetes* 43:329–336, 1994
17. Mirzabekov TA, Lin M, Kagan BL: Pore formation by the cytotoxic islet amyloid peptide amylin. *J Biol Chem* 271:1988–1992, 1996
18. Ricordi C, Scharp DW: Reversal of diabetes in nude mice after transplantation of fresh and 7-day-cultured (24°C) human pancreatic islets. *Transplantation* 45:994–996, 1988
19. El-Naggar MM, Elayat AA, Ardawi MSM, Tahir M: Isolated pancreatic islets of the rat: an immunohistochemical and morphometric study. *Anat Rec* 237:489–497, 1993
20. Kudva YC, Mueske C, Butler PC, Eberhardt NL: A novel *in vitro* assay of human islet amyloid polypeptide amyloidogenesis and effects of insulin secretory vesicle peptides on amyloid formation. *Biochem J* 321:809–813, 1998
21. Hattori T, Hosokawa Y, Sugihara H, Fukuda M: DNA content of diffusely infiltrative carcinomas in the stomach. *Pathol Res Pract* 180:615–618, 1985
22. Jones KH, Senft JA: An improved method to determine cell viability by simultaneous staining with fluorescein diacetate-propidium iodide. *J Histochem Cytochem* 33:77–79, 1985
23. Pace CS, Sachs G: Glucose-induced proton uptake in secretory granules of β-cells in monolayer culture. *Am J Physiol* 242:C382–C387, 1982
24. Couce M, O'Brien TD, Moran A, Roche PC, Butler PC: Diabetes mellitus in cystic fibrosis is characterized by islet amyloidosis. *J Clin Endocrinol Metab* 81:1267–1272, 1996
25. McDowell EM, Trump BF: Histologic fixatives suitable for diagnostic light and electron microscopy. *Arch Pathol Lab Med* 100:405–414, 1976
26. Spurr AR: A low viscosity epoxy resin embedding medium for electron microscopy. *J Ultrastruct Res* 71:173–184, 1969
27. Howie SEM, Cotton GJ, Heslop I, Martin NJ, Harrison DJ, Ramage R: Synthetic peptides representing discontinuous CD4-binding epitopes of HIV-1 gp 120 that induce T cell apoptosis and block cell death induced by gp 120. *FASEB J* 12:991–998, 1998
28. Williams AJ: The measurement of the function of ion channels reconstituted into artificial membranes. In *Ion Channels, A Practical Approach*. Ashley RH, Ed. Oxford, U.K., IRL/Oxford University Press, 1995, p. 43–67
29. Berne BJ, Pecora R: *Dynamic Light Scattering*. New York, Wiley, 1976
30. Alvarez O: Setting up a bilayer system. In *Ion Channel Reconstitution*. C. Miller, Ed. New York, Plenum, 1986, p. 129
31. Higham CE, Lewis M, Morris JF, Clark A: Cytotoxicity of human islet amyloid polypeptide to β-TC cells is mediated via apoptosis and necrosis (Abstract). *Diabetologia* 655:A168, 1998
32. Davis-Salinas J, Van Nostrand WE: Amyloid β-protein aggregation nullifies its pathologic properties in cultured cerebrovascular smooth muscle cells. *J Biol Chem* 270:20887–20890, 1995
33. Westermark P: Fine structure of islets of Langerhans in insular amyloidosis. *Virchows Arch* 359:1–18, 1973
34. De Koning EJP, Morris ER, Hofhuis FMA, Posthuma G, Hoppener JW, Morris JF, Capel PJ, Clark A, Verbeek JS: Intra- and extracellular amyloid fibrils are formed in cultured pancreatic islets of transgenic mice expressing human islet amyloid polypeptide. *Proc Natl Acad Sci U S A* 91:8467–8471, 1994
35. Loo DT, Copani A, Pike CJ, Whittemore ER, Walencewicz AJ, Cotman CW: Apoptosis is induced by β-amyloid in cultured central nervous system neurons. *Proc Natl Acad Sci U S A* 90:7951–7955, 1993
36. Behl C, Davis JB, Klier FG, Schubert D: Amyloid β peptide induces necrosis rather than apoptosis. *Brain Res* 645:253–264, 1994
37. Schubert D, Behl C, Lesley R, Brack A, Dargusch R, Sagara Y, Kimura H: Amyloid peptides are toxic via a common oxidative mechanism. *Proc Natl Acad Sci U S A* 92:1989–1993, 1995
38. Behl C, Davis JB, Lesley R, Schubert D: Hydrogen peroxide mediates amyloid β protein toxicity. *Cell* 77:817–827, 1994
39. Dypbukt JM, Ankarcrona M, Burkitt M, Sjoholm A, Strom K, Orrenius S, Nicotera P: Different prooxidant levels stimulate growth, trigger apoptosis, or produce necrosis of insulin-secreting RINm5F cells. *J Biol Chem* 269:30553–30560, 1994